A Fuzzy C-means Clustering Algorithm for Image Segmentation Using Nonlinear Weighted Local Information

Jian-Hua Song

College of Automation, Harbin Engineering University, Harbin 150001, China
Electronic Engineering College, Heilongjiang University, Harbin 150080, China
98dg_sjh@163.com

Wang Cong and Jin Li*

College of Automation,Harbin Engineering University, Harbin, 150001, China
cwcy9156@163.com; lijin@hrbeu.edu.cn
*Corresponding author: lijin@hrbeu.edu.cn

ABSTRACT. *Fuzzy c-means (FCM) clustering technique has been widely applied in image segmentation. However, it is quite sensitive to the various noises or outliers. In order to further improve the segmentation accuracy and robustness to noise, a fuzzy nonlinear weighted local information c-means clustering method is proposed for unsupervised segmentation of noisy images in this paper. First, a fuzzy nonlinear weighted factor including both the spatial distance of local window and its gray-level difference in the similarity measure is introduced to guarantee noise insensitiveness. Second, the spatial neighbor constraints are also taken in the membership function to enhance fuzzy clustering performance. The performance of this algorithm is evaluated by two images: synthetic images and brain MR images, and the experimental results demonstrate that the proposed algorithm is more robust to noise and effectively preserves the image detail than FCM algorithm and its variants.*

Keywords: Image segmentation, Nonlinear weighted, Fuzzy c-means clustering, Spatial constraints

1. **Introduction.** Image segmentation is a basic computer vision technology, and it is one of key steps in image processing and analysis. At present, many methods have been presented and applied to image segmentation, such as thresholding method [1, 2, 3], Markov random field method [4, 5], region growing method [6, 7], watershed method [8, 9] and clustering method [10], etc. In view of the advantages of fuzzy clustering algorithm, it has been widely adopted in image segmentation [11, 12].

Fuzzy c-means(FCM) clustering algorithm describes the membership relation between different object and background using mathematical method, the soft classification result is more credible and reasonable, and the theoretical system of fuzzy clustering is very mature. However, there are many drawbacks in FCM clustering algorithm, for example, FCM is quite sensitive to noise and outliers for lacking spatiotemporal correlation of local neighborhood in the image. To avoid those shortcomings in the process of image segmentation, some literatures proposed the improved FCM algorithms combined with image spatial information in its objective function or similarity measure [13, 14, 15, 16, 17, 18]. Ahmed *et al.* [19] proposed an algorithm that incorporated the neighboring spatial

information of a pixel in local window into the objective function of the FCM algorithm to enhance anti-noise performance (called FCM_S). In order to extend the distance measure of data in multidimensional feature space and reduce the computational time, Chen *et al.* [20] designed two improved schemes: KFCM_S1 and KFCM_S2, in which the image is processed by mean and median filtering in advance, respectively, to simplify and expand the neighborhood term of FCM_S.

However, there is a key parameter α in the aforementioned algorithms, and it is used to maintain the relative balance between the unprocessed image and its filtered image. The control factor α is usually difficult to estimate, and it is achieved through trial-and-error experiments in most cases. To solve this problem, Krinidis *et al.* [21] presented a called FLICM (fuzzy local information c-means) clustering algorithm, which introduces an adaptive control factor in its objective function without trial-and-error experiments, as well as obtaining the better anti-noise performance and image segmentation accuracy. FLICM algorithm can use more local spatial information of the image, but it is still inadequate in spatial constraint between the center pixel and neighborhood pixels.

This paper proposed an improved spatial constraints clustering method, which can make full use of the characteristics of noise-resistibility, robustness and image detail preservation of FLICM algorithm, meanwhile we further integrate local spatial information of the image and put forward two improvements.

First, we introduce a nonlinear weighted fuzzy parameter depending on the spatial distance of local neighborhood pixels and their gray-level difference simultaneously. Second, the spatial neighboring constraints are incorporated into similarity measurement, as well as so do in the membership function. The experiments showed that the proposed algorithm could further enhance the segmentation accuracy and improve its anti-noise performance.

2. Method.

2.1. **Fuzzy local information c-means (FLICM).** FLICM algorithm employed an intelligent control factor G_{ki} which enhanced the similarity measure level of local neighborhood pixels in its objective function[21], and the fuzzy factor G_{ki} is defined as

$$G_{ki} = \sum_{\substack{j \in N_i \\ i \neq j}} \frac{1}{d_{ij}+1}(1-\mu_{kj})^m \|x_j - v_k\|^2 \tag{1}$$

where the center pixel of the local window is x_i, and x_j are the neighborhood pixels located in the window (N_i). k is the reference cluster, and v_k is the cluster center of the k-th cluster. μ_{kj} is the fuzzy membership degree of the j-th pixel belonging to the k-th cluster, d_{ij} denotes the spatial Euclid distance between the i-th pixel and j-th pixel. In Eq.(1), local spatial distance and gray level are incorporated into the fuzzy factor G_{ki}, and the objective function was defined as follows

$$J_{FLICM} = \sum_{i=1}^{N}\sum_{k=1}^{c}\left[\mu_{ki}^m\|x_i - v_k\|^2 + G_{ki}\right] \tag{2}$$

By minimizing Eq.(2) with respect to μ_{ki} and v_k can be derived, as shown in Eqs. (3)-(4)

$$\mu_{ki} = \frac{1}{\sum\limits_{j=1}^{c} \left[\frac{\|x_i - v_k\|^2 + G_{ki}}{\|x_i - v_j\|^2 + G_{ji}} \right]^{1/(m-1)}} \qquad (3)$$

$$v_k = \frac{\sum\limits_{i=1}^{N} \mu_{ki}^m x_i}{\sum\limits_{i=1}^{N} \mu_{ki}^m} \qquad (4)$$

A main advantage of FLICM is introduction of the factor G_{ki}. First, unlike the factor α in FCM_S and its variants, G_{ki} is a variable and can be automatically determined at any time with the change of local neighborhood window. Second, the parameter value is not solely obtained based on the spatial distance between the pixels, but the spatial distance and gray level of the pixels are taken into account. Third, FLICM algorithm can be directly applied in image segmentation without preprocessing steps. However, there are also some drawbacks in FLICM algorithm. According to the analysis of literature [22], the spatial distance in fuzzy factor G_{ki} used to estimate the similarity measure between neighbor pixels is unreasonable in some cases.

2.2. **Proposed Method.** In order to further weaken the influence of corrupted image by all kinds of noise, and overcome the shortcomings of fuzzy factor G_{ki}, we design a novel factor of local similarity measure w_{ki}, which is adopted to replace the spatial distance. The factor w_{ki} is composed of the spatial distance measure (called $w_{s_{ij}}$) and the local gray-level relationship (called $w_{g_{ij}}$)), it is defined after normalization as shown below

$$w_{ij} = \frac{w_{s_{ij}} w_{g_{ij}}}{\sum w_{s_{ij}} w_{g_{ij}}} \qquad (5)$$

where the center pixel of the local window is the i-th pixel, and the definitions of $w_{s_{ij}}$ and $w_{g_{ij}}$ are given as follows

$$w_{s_{ij}} = \exp\left[-\frac{(p_j - p_i)^2 + (q_j - q_i)^2}{\sum\limits_{j \in N_i} [(p_j - p_i)^2 + (q_j - q_i)^2]} \right] \qquad (6)$$

$$w_{g_{ij}} = \exp\left[-\frac{(g_j - g_i)^2}{\lambda_{ij}^2} \right] \qquad (7)$$

where (p_i, q_i) and (p_j, q_j) are the spatial coordinate of the i-th pixel and j-th pixel respectively, g_i is grey-scale value of the center pixel within a pre-specified window, g_j is grey-scale value of the j-th pixel falling into the same window, λ_{ij} is the adaptive intensity factor of local window, as shown in Eq.(8).

$$\lambda_{ij} = \sqrt{\frac{\sum\limits_{j \in N_i} (g_j - g_i)^2}{N_R}} \qquad (8)$$

To acquire more local context information, the factor S_{ki}, a variant of the factor G_{ki}, utilizes the weighted parameter with spatial and gray distance to substitute for the simple spatial distance, and it is defined as follows

$$S_{ki} = \sum_{\substack{j \in N_i \\ i \neq j}} \frac{(1 - \mu_{kj})^m \|x_j - v_k\|^2}{1 + w_{ij}} \qquad (9)$$

In factor G_{ki}, it is unreasonable that distance measure d_{ij} considers only the difference of spatial distance between the central pixel and neighbor pixels in the same window, while ignoring the effect of the gray level difference between them. Therefore, a fuzzy factor S_{ki} is defined to denote comprehensively the local neighborhood relationship in Eq.(9). After calculated the new factor S_{ki}, to replace G_{ki} in Eq.(2), the new object function is described as follow

$$J_m = \sum_{i=1}^{N} \sum_{k=1}^{c} \left[\mu_{ki}^m \|x_i - v_k\|^2 + \sum_{\substack{j \in N_i \\ i \neq j}} \frac{(1 - \mu_{kj})^m \|x_j - v_k\|^2}{1 + w_{ij}} \right] \tag{10}$$

By minimizing Eq.(10), the membership degree matrix μ_{ki} and the prototypes of the clusters v_k are obtained as follows

$$\mu_{ki} = \sum_{j=1}^{c} \left[\frac{\|x_i - v_k\|^2 + S_{ki}}{\|x_i - v_j\|^2 + S_{ji}} \right]^{-1/(m-1)} \tag{11}$$

$$v_k = \frac{\sum\limits_{i=1}^{N} \mu_{ki}^m x_i}{\sum\limits_{i=1}^{N} \mu_{ki}^m} \tag{12}$$

Besides adopting nonlinear weighted distance measure in object function, in order to improve the performance of fuzzy clustering, another improvement is that the membership degree μ_{ki} is modified based on the similar characteristics of the local window [15, 23]. First, the local neighborhood distance d_{ij} is introduced into membership degree μ_{ki} in Eq.(11), the new membership degree h_{ki} is more reasonable for considering neighbor information, and then normalization processing h_{ki} using Eq.(13).

$$h_{ki} = \frac{\sum\limits_{j \in N_i} (\mu_{ij}/d_{ij})}{\sum\limits_{j \in N_i} d_{ij}} \tag{13}$$

$$\mu_{ki}^* = \frac{\mu_{ki} h_{ki}}{\sum\limits_{j=1}^{c} \mu_{ji} h_{ji}} \tag{14}$$

In Eq.(14), μ_{ki}^* represents the normalization degree of membership ($\mu_{ki}^* \in [0,1]$, $\sum_{k=1}^{c} \mu_{ki}^* = 1$ and $\sum_{i=1}^{N} \mu_{ki}^* < N$), c denotes the number of cluster. $d_{ij} = (p_j - p_i)^2 + (q_j - q_i)^2$ is the squared Euclidean distance between the coordinates of pixel x_i and its neighborhood pixels x_j, (p_j, q_j) and (p_i, q_i) are the coordinates x_j and x_i in the image, respectively. In Eq.(13), $1/d_{ij}$ is the reciprocal of the distance d_{ij}, because the neighborhood pixel x_j is the nearer to the center pixel x_i, the greater the effect to the membership degree, and vice versa.

The FNWLICM algorithm can be summarized as follows:

Step 1: set the number of cluster c, the exponent of fuzziness m, the size of local neighborhood window and stop criterion ε.

Step 2: initialize randomly the fuzzy cluster prototypes $V^{(1)} = \{v_1^{(1)}, v_2^{(1)}, \cdots, v_c^{(1)}\}$, and set the loop counter $b = 0$.

Step 3: compute the parameter of local similarity measure w_{ij}.

Step 4: update the membership degree μ_{ki} by Eq.(11).

Step 5: compute and update the new membership degree μ_{ki}^* by Eq.(14).

Step 6: compute and update the cluster center v_k by Eq.(12)(μ_{ki} is replaced by μ_{ki}^*).

Step 7: If max $|V^{(b+1)} - V^{(b)}| < \varepsilon$ then stop, otherwise, set $b = b+1$ and go to step 3.

3. **Experimental results.** In experiments, we chose two images: (a) synthetic image, (b) medical Magnetic Resonance (MR) image. In order to validate the validity of the FNWLICM algorithm, several typical segmentation methods based on FCM or its variants are used as compared methods such as FCM, FCM_S, FCM_S1, FCM_S2, and FLICM. In this section, we set the fuzzy weighting exponent $m = 2$, the stopping condition $\varepsilon = 0.001$, the size of the neighborhood window is 3×3 in all experiments.

3.1. **Experimental results on synthetic images.** Fig.1(a) is an artificial synthetic image with 128×128 pixels, and its grey value has two intensity level taken as 20 and 230. To test the anti-noise performance of the proposed algorithm, salt and pepper noise (20%) is added in the synthetic image, and the noisy image is segmented into two classes by six fuzzy clustering algorithms, respectively. The segmentation results are shown in Fig.1(c)-Fig.1(h). In order to further quantitatively to analyze the segmentation performance, the misclassification rate (MCR) of six algorithms with different noise levels is shown in Table 1. MCR is a performance indicator, and it is defined as follows

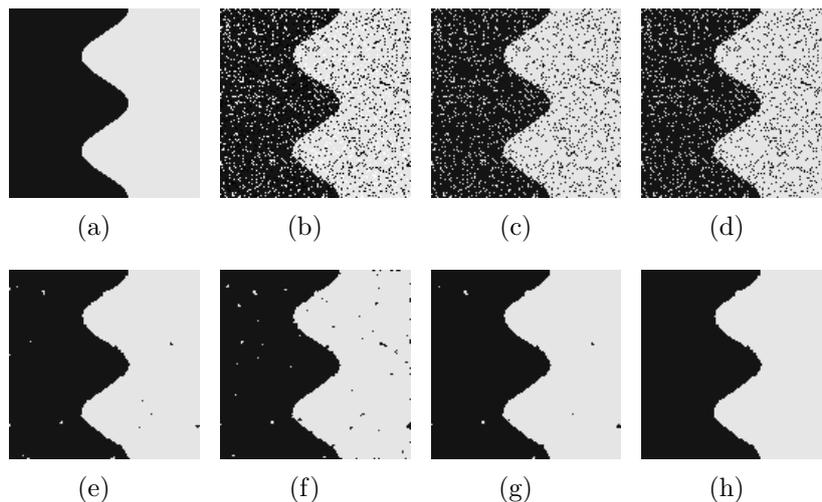$$MCR = \frac{total \; number \; of \; misclassified \; pixels}{total \; number \; of \; pixels} \tag{15}$$

FIGURE 1. Segmentation results of salt and pepper noise-corrupted synthetic image. (a) original image, (b) noisy image, (c) FCM, (d) FCM_S, (e) FCM_S1, (f) FCM_S2, (g) FLICM and (h) FNWLICM

It is intuitively seen from Fig.1 that FNWLICM algorithm has the best segmentation result in all six fuzzy clustering algorithms, and other algorithms more or less are influenced by salt and pepper noise. It is also shown from the specific experimental data in Table 1, MCR values of FNWLICM algorithm are still minimum compared with other segmentation algorithms when changing the level of noise.

Furthermore, the experimental result of the second synthetic image is shown in Fig.2. The size of synthetic image is also 128×128, it contains two gray values taken as 30 and 220, as shown in Fig.2(a). Now the original image is corrupted by 25% Gaussian noise, as shown in Fig.2(b). The conclusion is similar to Fig.1, namely FNWLICM algorithm is still optimal. It is noticed that the segmentation results of FCM and FCM_S are unacceptable, the noise hasnt been removed, most of the noise is still remained in image, and the segmentation results of other algorithms such as FCM_S1, FCM_S2 and FLICM are also

TABLE 1. Comparison of MCR on noise-corrupted synthetic image

Levels of Noise (%)	FCM	FCM_S	FCM_S1	FCM_S2	FLICM	FNWLICM
10	0.0536	0.0370	0.0012	0.0018	0.0014	0.0012
15	0.0742	0.0467	0.0024	0.0045	0.0025	0.0019
20	0.1037	0.0576	0.0048	0.0094	0.0044	0.0027
25	0.1213	0.0695	0.0052	0.0118	0.0046	0.0040
30	0.1479	0.0804	0.0076	0.0204	0.0063	0.0059
35	0.1757	0.0883	0.0145	0.0391	0.0128	0.0097
40	0.2021	0.0965	0.0284	0.0626	0.0262	0.0174

dissatisfactory. Obviously, FNWLICM algorithm can remove almost all the Gaussian noise, and its anti-noise performance is the most satisfactory, as shown in Fig.2(h).
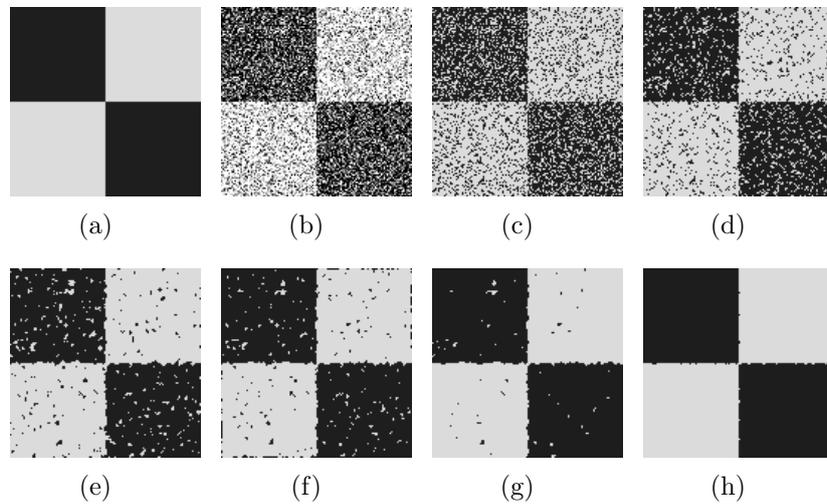

FIGURE 2. Segmentation results of Gaussion noise-corrupted image. (a) Original image, (b) noisy image, (c) FCM, (d) FCM_S, (e) FCM_S1, (f) FCM_S2, (g) FLICM and (h) FNWLICM

Similarly, we also calculate the averaged misclassification rate of the six clustering algorithms with different levels of Gaussian noises (10%, 15%, 20%, 25%, 30%, 35% and 40%), as shown in Fig.3, here taking MCR and the level of noise as vertical and horizontal coordinates, respectively. It is can be seen that with the level of noise increasing MCR of six algorithms is gradually ascending, but MCR values of FNWLICM algorithm always less than the others.

3.2. **Experimental results on brain MR image.** In this section, firstly, the simulated brain MR images from BrainWeb images [25] is used in the experiments to compare the performance of the previous six algorithms. The T1-weighted brain MR image has 181×217 pixels with slice thickness of 1 mm, its cranium and blood vessels have been dislodged before cluster processing. The MR image is corrupted by 15% Rician noise and no intensity in homogeneities, as shown in Fig.4(a). In general, the brain tissue is very complex, but it can be usually regard as three classes: grey matter (GM), white matter (WM) and cerebrospinal fluid (CSF). In our experiments, MR image is segmented into four classes (the background is included), and the segmentation results using the six methods are shown in Fig.4, respectively.
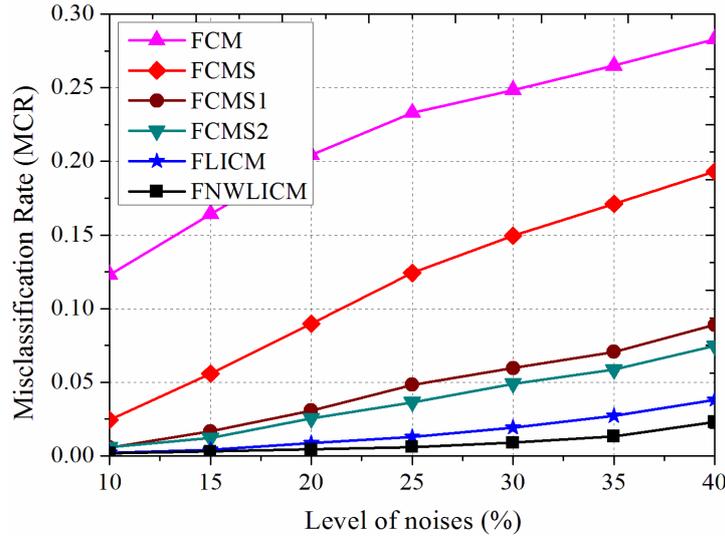
FIGURE 3. The curve diagram of *MCR* of six algorithms on Gaussian noise-corrupted image

Fig.4(a) is the brain MR image with 15% (l=15) Rician noise, Fig.4(c)-Fig.4(h) are the binary images of CSF, WM and GM after the image is segmented by six algorithms, respectively. It can be observed from Fig.4 that FNWLICM algorithm is more superior to other algorithms on the extraction of brain tissue, and the other five algorithms are inaccurate on the segmentation from noisy MR image.

In order to quantitative analysis the anti-noise performance of six algorithms, 6 brain MR images (the level of Rician noise ranges from 5% to 20%) are selected as the experimental samples. The statistical results (average values) of the Jaccard Similarity (*JS*)[26] values of GM, WM and CSF are showed in Table 2. *JS* was used for comparison and quantitative evaluation.

$$JS = \frac{|A_i \cap B_i|}{|A_i \cup B_i|} \tag{16}$$

where A_i denotes the set of pixels belonging to the i-th class identified by the clustering algorithm, while B_i denotes the set of pixels belonging to the i-th class in the groundtruth. As a fuzzy similarity measure, the larger the *JS* value, the better the clustering performance is. It can be seen from the experimental results in Table 2, with the increase of noise level of MR image, *JS* values of the all algorithms are reduced. However, FN-WLICM algorithm has higher values than the other five algorithms, and it illustrates that the proposed algorithm has a better anti-noise ability and higher segmentation accuracy.

To further verify the performance of the algorithm, a real clinical normal MR image was selected from the Whole Brain Atlas clinical MR image database. Fig.5(a) is a T1-weighted MR image, the segmentation results of MR image are shown in Fig.5(b) - Fig.5(g). It can be seen from the experiment results that the proposed algorithm can effectively maintain the region homogeneity, as well as preserve more detail information of the original MR image. Although other algorithms can also overcome most of the interference, there exists misclassification in segmented images where a small amount of white matter was processed as a part of the gray matter.

4. **Conclusions.** In this work, we have proposed a fuzzy nonlinear weighted local information c-means (FNWLICM) method on unsupervised image segmentation, and it is in fact an improved FLICM method. One of the core ideas of FNWLICM algorithm is to
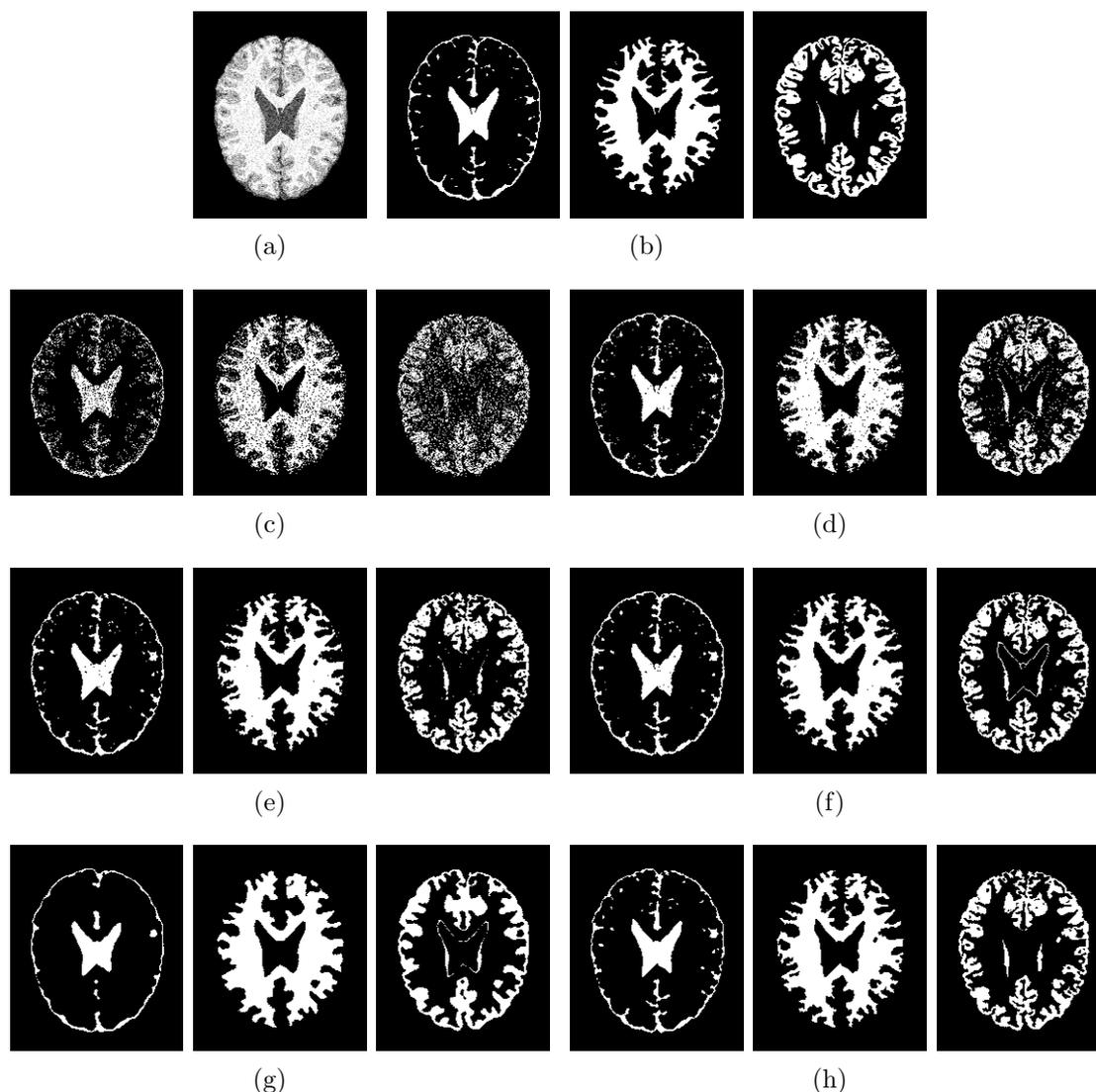
FIGURE 4. Segmentation results of the six methods on the MR image with 15% Rician noise. (a) noisy MR image, (b)ground truth, (c) FCM, (d) FCM_S, (e) FCM_S1, (f) FCM_S2, (g) FLICM and (h) FNWLICM.

combine both the local spatial neighborhood information and gray-level information in similarity measure with nonlinear weighted form, this similarity measure can more accurately described the spatial constraint relation of center pixel and its neighbor pixels in the same window. In addition, the membership values are also adjusted with local neighborhood information, and the updated membership values contribute to the improvement of clustering performance. In experiments, we have quantitative and qualitative comparison and analysis between the proposed algorithm and other five algorithms (FCM, FCM_S, FCM_S1, FCM_S2 and FLICM) for synthetic images, brain MR images. All experimental results demonstrated the presented algorithm has higher segmentation accuracy, and can effectively resist all kind of noises and outliers.

TABLE 2. Comparison of *JS* on simulated MR images with different level of noises

Algorithm	Tissues	5%	10%	15%	20%
FCM	WM	0.8293	0.7676	0.7194	0.6274
	GM	0.6899	0.6197	0.5440	0.4863
	CSF	0.7239	0.6671	0.6103	0.5501
FCM_S	WM	0.8875	0.8383	0.7950	0.7271
	GM	0.7704	0.7371	0.7051	0.6468
	CSF	0.8068	0.7564	0.7171	0.6619
FCM_S1	WM	0.9095	0.8868	0.8578	0.8056
	GM	0.7816	0.7597	0.7281	0.6927
	CSF	0.8458	0.8104	0.7874	0.7573
FCM_S2	WM	0.9243	0.9025	0.8746	0.8281
	GM	0.8236	0.8024	0.7707	0.7414
	CSF	0.8293	0.7957	0.7622	0.7346
FLICM	WM	0.9013	0.8720	0.8334	0.8003
	GM	0.8045	0.7723	0.7311	0.6927
	CSF	0.8457	0.8006	0.7705	0.7432
FNWLICM	WM	0.9591	0.9380	0.9147	0.8885
	GM	0.9125	0.8793	0.8489	0.8017
	CSF	0.9017	0.8675	0.8321	0.7937

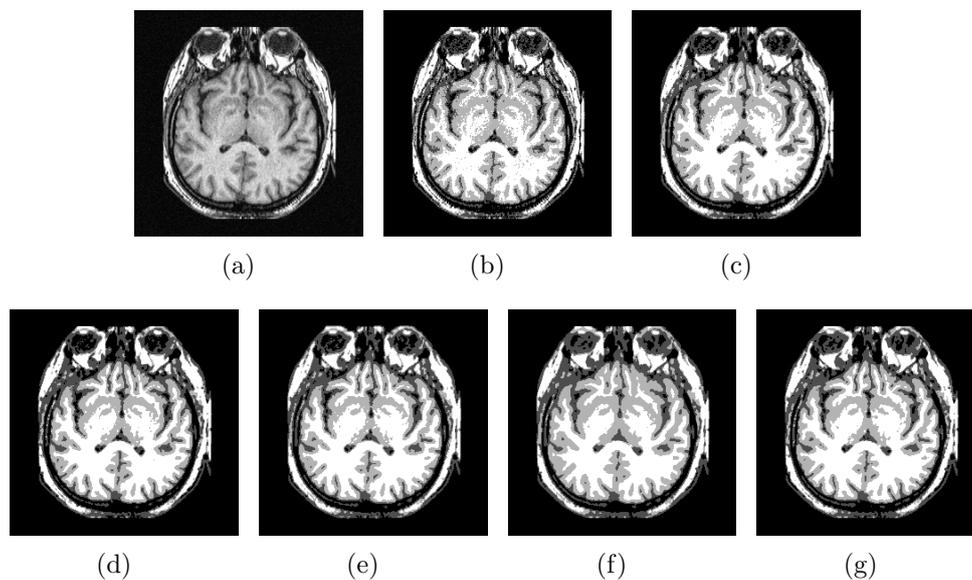

FIGURE 5. Segmentation results on real MR image. (a) MR image (b) FCM (c) FCM_S (d) FCM_S1 (e) FCM_S2 (f) FLICM and (g) FNWLICM

REFERENCES

[1] S. K. Choy, M. L. Tang, and C. S. Tong. Image Segmentation Using Fuzzy Region Competition and Spatial/Frequency Information, *IEEE Transactions on Image Processing*, vol.20, no.6, pp.1473–1484, 2011.

[2] P. D. Sathya, and R. Kayalvizhi, Modified bacterial foraging algorithm based multilevel thresholding for image segmentation, *Engineering Applications of Artificial Intelligence*, vol.24, no.4, pp.595-615, 2011.

[3] K. S. Tan, and N. A. M. Isa, Color image segmentation using histogram thresholding C Fuzzy C-means hybrid approach, *Pattern Recognition*, vol.44, no.1, pp.1-15, 2011.

[4] C. Zheng, Q. Qin, G. Liu, and Y. Hu, Image segmentation based on multiresolution Markov random field with fuzzy constraint in wavelet domain. *IET Image Processing*, vol.6, no.3, pp.213-221, 2012.

[5] S.Ribes, D. Didierlaurent, N. Decoster, E. Gonneau, and L. Risser, Automatic Segmentation of Breast MR Images Through a Markov Random Field Statistical Model. *IEEE Transactions on Medical Imaging*, vol.33, no.10, pp.1986-1996, 2014.

[6] P. Yu , A. K. Qin, and D. A. Clausi, Unsupervised Polarimetric SAR Image Segmentation and Classification Using Region Growing With Edge Penalty, *IEEE Transactions on Geoscience and Remote Sensing*, vol.50, no.4, pp.1302-1317, 2012.

[7] L. Zhu, Y. Gao, and A. Yezzi, Automatic Segmentation of the Left Atrium from MR Images via Variational Region Growing With a Moments-Based Shape Prior, *IEEE Transactions on Image Processing*, vol.22, no.12, pp.5111-5122, 2013.

[8] Y. Tarabalka, J. Chanussot and J. A. Benediktsson, Segmentation and classification of hyperspectral images using watershed transformation. *Pattern Recognition*, vol.43, no.7, pp.2367-2379, 2010.

[9] W. Y. Hsu, Improved watershed transform for tumor segmentation Application to mammogram image compression. *Expert Systems with Applications*, vol.39, no.4, pp.3950-3955, 2012.

[10] R. Dubes, A. K. Jain, Clustering techniques: the user's dilemma, *Pattern Recognition*, vol.8, no.4, pp.247-260, 1976.

[11] Y. A. Tolias, S. M. Panas, Panas. Image segmentation by a fuzzy clustering algorithm using adaptive spatially constrained membership functions, *IEEE Transactions on Systems, Man, and Cybernetics-Part A: Systems and Humans*, vol.28, no.3, pp.359-369, 1998.

[12] S. Kala, and S. Vasuki, Feature correlation based parallel hyper spectral image compression using a hybridization of FCM and subtractive clustering, *Journal of Communications Technology and Electronics*, vol.59, no.12, pp.1378-1389, 2014.

[13] W. Cong , J. H. Song, L. Wang, H. Liang, and J. Li, A Fuzzy C-Means Clustering Scheme Incorporating Non-Local Spatial Constraint for Brain Magnetic Resonance Image Segmentation, *Journal of Medical Imaging and Health Informatics*, vol.5, no.8, pp.1281-1285, 2015.

[14] W. Cai, S. Chen, and D. Zhang, Fast and robust fuzzy c-means clustering algorithms incorporating local information for image segmentation. *Pattern Recognition*, vol.40, no.3, pp.825-838, 2007.

[15] X. Y. Wang, and J. Bu, A fast and robust image segmentation using FCM with spatial information. *Digital Signal Processing*, vol.20, no.4, pp.1173-1182, 2010.

[16] M. Gong, Y. Liang, J. Shi, W. Ma, and J. Ma, Fuzzy C-Means Clustering With Local Information and Kernel Metric for Image Segmentation, *IEEE Transactions on Image Processing*, vol.22, no.2, pp.573-584, 2013.

[17] I. Despotovic, E. Vansteenkiste, and W. Philips, Spatially Coherent Fuzzy Clustering for Accurate and Noise-Robust Image Segmentation, *IEEE Signal Processing Letters*, vol.20, no.4, pp.295-298, 2013.

[18] Z. Zhao, L. Cheng, and G. Cheng, Neighbourhood weighting fuzzy c-means clustering algorithm for image segmentation, *IET Image Processing*, vol.8, no.3, pp.150-161, 2014.

[19] M. N. Ahmed, S. M. Yamany, N. Mohamed, A. A. Farag, and T. Moriarty, A Modified Fuzzy C-Means Algorithm for Bias Field Estimation and Segmentation of MRI Data, *IEEE Transactions on Medical Imaging*, vol.21, no.3, pp.193-199, 2002.

[20] S. Chen, and D. Zhang, Robust Image Segmentation Using FCM With Spatial Constraints Based on New Kernel-Induced Distance Measure, *IEEE Transactions on Systems, Man, and Cybernetics-Part B: Cybernetics*, vol.34, no.4, pp.1907-1916, 2004.

[21] S. Krinidis, and V. Chatzis, A Robust Fuzzy Local Information C-Means Clustering Algorithm, *IEEE Transactions on Image Processing*, vol.19, no.5, pp.1328-1337, 2010.

[22] M. Gong, Z. Zhou, and J. Ma, Change detection in synthetic aperture radar images based on image fusion and fuzzy clustering. *IEEE Transactions on Image Processing*, vol.21, no.4, pp.2141-2151, 2012.

[23] N. Li, H. Huo, Y. M. Zhao, X. Chen, and T. Fang, A Spatial Clustering Method With Edge Weighting for Image Segmentation, *IEEE Transactions on Geoscience and Remote Sensing Letters*, vol.10, no.5, pp.1124-1128, 2013.

[24] C. Li, R. Huang, Z. Ding, J. C. Gatenby, and D. N. Metaxas, A level set method for image segmentation in the presence of intensity inhomogeneities with application to MRI, *IEEE Transactions on Image Processing*, vol.20, no.7, pp.2007-2016, 2011.

[25] D.L. Collins, A.P. Zijdenbos, V. Kollokian, J.G. Sled, N.J. Kabani, C.J. Holmes, and A.C. Evans, Design and Construction of a Realistic Digital Brain Phantom, *IEEE Transactions on Medical Imaging*, vol.17, No.3, pp.463–468, 1998.

[26] F. Masulli, and A. Schenone, A fuzzy clustering based segmentation system as support to diagnosis in medical imaging, *Artificial Intelligence in Medicine*, vol.16, no.2, pp.129-147, 1999.